

This article was downloaded by:

On: 25 January 2011

Access details: *Access Details: Free Access*

Publisher *Taylor & Francis*

Informa Ltd Registered in England and Wales Registered Number: 1072954 Registered office: Mortimer House, 37-41 Mortimer Street, London W1T 3JH, UK



## Liquid Crystals

Publication details, including instructions for authors and subscription information:

<http://www.informaworld.com/smpp/title~content=t713926090>

### Collective and non-collective excitations in antiferroelectric and ferroelectric liquid crystals studied by dielectric relaxation spectroscopy and electro-optic measurements

M. Buivydas; F. Gouda; G. Andersson; S. T. Lagerwall; B. Stebler; J. Bomelburg; G. Heppke; B. Gestblom

Online publication date: 29 June 2010

**To cite this Article** Buivydas, M. , Gouda, F. , Andersson, G. , Lagerwall, S. T. , Stebler, B. , Bomelburg, J. , Heppke, G. and Gestblom, B.(1997) 'Collective and non-collective excitations in antiferroelectric and ferroelectric liquid crystals studied by dielectric relaxation spectroscopy and electro-optic measurements', *Liquid Crystals*, 23: 5, 723 – 739

**To link to this Article:** DOI: 10.1080/026782997208000

**URL:** <http://dx.doi.org/10.1080/026782997208000>

PLEASE SCROLL DOWN FOR ARTICLE

Full terms and conditions of use: <http://www.informaworld.com/terms-and-conditions-of-access.pdf>

This article may be used for research, teaching and private study purposes. Any substantial or systematic reproduction, re-distribution, re-selling, loan or sub-licensing, systematic supply or distribution in any form to anyone is expressly forbidden.

The publisher does not give any warranty express or implied or make any representation that the contents will be complete or accurate or up to date. The accuracy of any instructions, formulae and drug doses should be independently verified with primary sources. The publisher shall not be liable for any loss, actions, claims, proceedings, demand or costs or damages whatsoever or howsoever caused arising directly or indirectly in connection with or arising out of the use of this material.

# Collective and non-collective excitations in antiferroelectric and ferroelectric liquid crystals studied by dielectric relaxation spectroscopy and electro-optic measurements

by M. BUIVYDAS\*, F. GOUDA†, G. ANDERSSON, S. T. LAGERWALL,  
B. STEBLER

Physics Department, Chalmers University of Technology, S-412 96 Göteborg, Sweden

† Physics Department, Umm Al-Qura University, Makkah, P.O. Box 715,  
Saudi Arabia

J. BOMELBURG, G. HEPPE

Iwan-N.-Stranski-Institut, Technische Universität Berlin, Sekr. ER 11,  
Str. des 17. Juni 135, D-10623 Berlin, Germany

and B. GESTBLOM

Physics Department, Uppsala University, S-751 21 Uppsala, Sweden

(Received 24 December 1996; in final form 7 April 1997; accepted 16 June 1997)

The dynamics of different molecular modes in four antiferroelectric liquid crystal substances have been studied by a combination of spectroscopic methods. The fastest motion is the reorientation around the molecular long axis, here found in the low GHz range by time domain spectroscopy. The reorientation around the short axis has a characteristic frequency of about 10 kHz and is detected by frequency domain spectroscopy in the homeotropic configuration. As for the collective excitations, the Goldstone and soft modes, characteristic of the ferroelectric phase, have counterparts in the antiferroelectric phase which appear very different. There are two characteristic peaks in the spectrum, one at high frequency, about 100 kHz, the other at low frequency, about 10 kHz. The latter has often been mistaken for short axis reorientation and both have been attributed to soft modes. By combining different experimental techniques and different geometries it can be shown that neither is a soft mode, but both are collective modes of different character: the high frequency mode corresponds to fluctuations where molecules in neighbouring layers are moving in opposite phase, the low frequency mode to phase fluctuations in the helicoidal superstructure. In materials exhibiting a C\* phase in addition to the C<sub>a</sub>\* or C<sub>γ</sub>\* phases, an additional strong peak appears in at least one lower-lying phase adjacent to the C\* phase. We show that this peak, which we call a hereditary peak, has nothing to do with the antiferroelectric or ferroelectric order, but is just the Goldstone peak from a coexisting C\* phase. In the same way, a Goldstone mode peak from the C<sub>γ</sub>\* phase may appear in the underlying C<sub>a</sub>\* phase. In a general way, narrow phases like C<sub>γ</sub>\*, being bounded by first order transitions on both sides (C<sub>a</sub>\*–C<sub>γ</sub>\*–C\*) are likely to show non-characteristic (hereditary) peaks from both adjacent phases.

## 1. Introduction

The new phenomena of ferroelectricity [1, 2], paraelectricity [3], antiferro- and ferri-electricity [4] have greatly stimulated research in chiral smectics. In the antiferroelectric smectic C\* (C<sub>a</sub>\*) phase, the molecules in the neighbouring layers are tilted from the layer normal in opposite or almost opposite [5] directions. Materials exhibiting antiferroelectric phases possess different sequences of tilted smectic phases where the most often observed is A\* → C<sub>α</sub>\* → C\* → C<sub>γ</sub>\* → C<sub>a</sub>\* where

A\*, C\* and C<sub>γ</sub>\* are the paraelectric smectic A\*, ferroelectric C\* and ferroelectric C\* phases, respectively [6]. The transitions from the C\* to C<sub>γ</sub>\* and from the C<sub>γ</sub>\* to C<sub>a</sub>\* are first order [7–9]. This fact, together with the narrow temperature range of the C<sub>γ</sub>\* phase, has important implications for the observed properties and their interpretations.

Dielectric relaxation spectroscopy (DRS) is a powerful tool for studying the molecular dynamics in these systems because it covers a broad frequency range of 15 orders of magnitude (10<sup>-3</sup>–10<sup>12</sup> Hz). Thus the DRS technique has the ability to follow collective and

\* Author for correspondence.

non-collective molecular processes. As an example of a collective process, in the paraelectric  $A^*$  phase, the dielectric permittivity  $\epsilon$  has a contribution from the director tilt fluctuations (soft mode). In the ferroelectric  $C^*$  phase  $\epsilon$  has, besides the soft mode, another collective mode due to phase fluctuations (Goldstone mode). The Goldstone mode is characterized by a relaxation frequency which, for most of the compounds investigated so far, does not exceed a few kHz. On approaching the  $A^*$  to  $C^*$  transition, the soft mode dielectric strength  $\epsilon_s$  peaks and its relaxation frequency  $f_s$  softens, i.e. it exhibits a critical slowing down. While the dynamics of the soft and Goldstone modes in the paraelectric and ferroelectric chiral smectics have been extensively investigated by a variety of groups [10–15], the excitations observed in the ferroelectric and antiferroelectric phases are poorly characterized and understood, and their molecular aspects a subject of controversy [8, 16–28].

The dielectric spectrum of the antiferroelectric  $C_a^*$  phase exhibits two characteristic absorption peaks ( $P_L, P_H$ ) [8, 23–26] observed in the kHz and MHz range, respectively. The  $P_L$  process has been attributed [24] to an antiferroelectric soft mode, but other authors [8, 23–25] have interpreted this process as the molecular reorientation around the short axis. The molecular origin of the  $P_H$  process is also controversial. A soft mode interpretation has been proposed [23], and other authors [24–26] have assigned this process to a distortion of the antiferroelectric ordering—the reorientation of the molecules in two adjacent smectic layers in an *opposite* unwinding fashion. An attempt has also been made to relate the  $P_H$  absorption to the helicoidal superstructure [8]. As for the  $P_L$  absorption we have, in our previous work [26], been able to exclude the possibility that  $P_L$  is connected with the molecular reorientation around the short axis; instead, we interpret it as a phase fluctuation in the helicoidal superstructure.

In the dielectric spectrum of the ferroelectric  $C_\gamma^*$  phase

there is a low frequency absorption ascribed [8, 23–28] to a Goldstone mode. A high frequency peak has also been observed in the  $C_\gamma^*$  phase [23, 26–28] and attributed [26] to a soft mode. The aim of the present work is to clarify the molecular origin of these multiple absorption peaks observed in the  $C_\gamma^*$  and  $C_a^*$  phases.

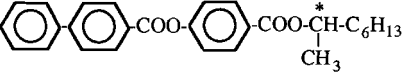
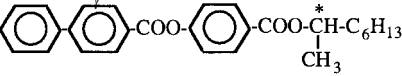
## 2. Materials

The investigated materials are listed in the table. Except for LC1, which is commercially available, they have been prepared by the authors. All four materials possess  $C_\gamma^*$  and  $C_a^*$  phases. The temperature interval of  $C_\gamma^*$  in LC1 and LC2 is about  $1^\circ$ , whereas in LC3 and LC4 (single compounds), the  $C_\gamma^*$  phase extends over  $8^\circ$  and  $2^\circ$ , respectively. In LC3 and LC4, the two phases are preceded by a  $C^*$  phase, while the  $C^*$  phase is lacking in the LC1 and LC2 mixtures. The LC3 and LC4 compounds also exhibit a high order antiferroelectric phase ( $I_h^*$ ). Detailed dielectric data on LC1 (Chisso CS-4000) have been published elsewhere [26]. Like LC2, a five-component mixture whose composition and properties are described in references [29, 30], LC1 has been engineered to give the broadest possible range of the antiferroelectric phase.

## 3. Experimental

In order to cover the frequency range from 10 Hz to 10 GHz, two different measurement systems were employed. In the frequency range 10 Hz to 10 MHz the Hewlett-Packard impedance analyser (HP-4192A) was used. The high frequency realm, 10 MHz to 10 GHz, has been covered using time domain spectroscopy [31]. Most of our discussion will be focused on the molecular processes observed in the frequency regime 10 Hz to 10 MHz. The high frequency measurements have been carried out on LC1. Phase transition temperatures were checked using dielectric and polarizing microscope measurements.

Table

| Acronym | Transition temperatures $^\circ\text{C}$                                                                                                                                                                                                 |
|---------|------------------------------------------------------------------------------------------------------------------------------------------------------------------------------------------------------------------------------------------|
| LC1     | Low temperature antiferroelectric mixture (Chisso CS-4000)<br>I-100.0-A*-82.80-C $_\alpha^*$ -81.91-C $_\gamma^*$ -80.1-C $_\gamma^*$ -79.17-C $_a^*$ -10-Cr                                                                             |
| LC2     | Antiferroelectric mixture<br>I-131.5-A*-108-C $_\gamma^*$ -107-C $_a^*$ -35-Cr                                                                                                                                                           |
| LC3     | C $_{14}\text{H}_{29}$ -COO-  -COO-CH(CH $_3$ )-C $_6\text{H}_{13}$                                                                                  |
| LC4     | I-130.1-A*-116.0-C*-92.2-C $_\gamma^*$ -83.5-C $_a^*$ -53.5-I $_h^*$ -59.9-Cr<br>C $_{10}\text{H}_{21}$ -COO-  -COO-CH(CH $_3$ )-C $_6\text{H}_{13}$ |
|         | I-140.6-A*-117-C $_\alpha^*$ -115.1-C*-105.2-C $_\gamma^*$ -103.5-C $_a^*$ -68-I $_h^*$ -57.3-Cr                                                                                                                                         |

The dielectric measurements from 10 Hz to 10 MHz were carried out using planar and homeotropic geometries (the geometric designation given with reference to the A\* phase). The cell consisted of two glass plates coated with a conducting layer (indium tin oxide, ITO). Two thin layers of silicon monoxide were further evaporated onto each surface. The first layer was evaporated normal to the surface and used as an insulation layer to avoid breakdown of the cell at high fields. The dielectric measurements, in the planar orientation, were carried out on different cells of 2, 18 and 36  $\mu\text{m}$  thickness. In the planar case, a measuring electric field of 0.3 V<sub>pp</sub> was applied across the sample, usually in a direction parallel to the smectic layers. In order to study the electric field dependence of the dielectric permittivity and relaxation frequency, a bias electric field (0 to  $\pm 35$  V) was superimposed on the measuring field from the HP-4192 bridge.

The complex dielectric permittivity  $\varepsilon^*$  generally depends on the frequency ( $f$ ) of the measuring electric field, the temperature ( $T$ ) and the bias electric field ( $E$ ). We may write  $\varepsilon^*(f, T, E)$  as

$$\varepsilon^*(f, T, E) = \sum_R \frac{\varepsilon_R(T, E)}{1 + \left( j \frac{f}{f_R(T, E)} \right)^{1 - \alpha_R(T, E)}} + \varepsilon(\infty) \quad (1)$$

where  $\varepsilon_R$ ,  $f_R$  and  $\alpha_R$  refer to the dielectric strengths, relaxation frequencies and symmetric distribution parameters of the process in question. The high frequency dielectric permittivity  $\varepsilon(\infty)$  has contributions from high frequency processes such as electronic polarizability. The dielectric strength  $\varepsilon_R$  of each mode is defined as the difference between the dielectric permittivity measured at low and high frequencies of a relaxation region for the process in question. In previous papers we have used the symbol  $\Delta\varepsilon_R$  for the dielectric strength of a certain mode (a widespread habit), but feel a growing frustration because of unavoidable confusion with  $\Delta\varepsilon$  for dielectric anisotropy, one of the most firmly established symbols used in the literature. As dielectric studies very often involve both dielectric anisotropy  $\Delta\varepsilon$ , and dielectric biaxiality  $\delta\varepsilon$ , in addition to dielectric strength, we find it desirable to choose a different means of expression for the latter. Because the dielectric strength is essentially just a kind of renormalized dielectric constant (background subtracted) we feel that  $\varepsilon_R$  is appropriate and unlikely to be mistaken for anything else when used in the evident way ( $\varepsilon_S$ ,  $\varepsilon_G$ ,  $\varepsilon_H$ ,  $\varepsilon_L$ ... for soft, Goldstone mode, high, low frequency mode, etc.).

The measured dielectric absorption  $\varepsilon''$  contains, besides the multiple absorption peaks, a spurious contribution in the high frequency part of the spectrum due to the resistance of the ITO layer for which correction

has to be made (figure 1). In order to extract the correct values of  $\varepsilon_R$ ,  $f_R$  and  $\alpha_R$ , the imaginary part of the measured frequency dependence of  $\varepsilon''$  has been fitted to absorption peaks of Cole–Cole type

$$\varepsilon'' = \frac{\sigma}{2\pi\varepsilon_0} \left( \frac{1}{f^n} \right) + \sum_R \text{Im} \left( \frac{\varepsilon_R}{1 + \left( j \frac{f}{f_R} \right)^{1 - \alpha_R}} + \varepsilon(\infty) \right) + Af^m \quad (2)$$

where  $(\sigma/2\pi\varepsilon_0, n)$  and  $(A, m)$  are fitting parameters (exponents close to 1) of the low and high frequency contribution arising from the free charges and the ITO layer, respectively. The factor  $A$  depends on the time constant  $\tau$  of our cell, originating in the resistance of the ITO layer and the capacitance of the filled cell. For thinner cells, the cut-off frequency (or  $1/\tau$ ) will be lower than for thicker cells. This means that the contribution from the term  $Af^m$  in equation (2) will be more dominating at higher frequencies, which eventually may obscure an absorption peak due to a molecular process. Thus, in order to resolve a high frequency absorption in the dielectric spectrum, it is preferable to use thick cells. However, applying a bias voltage, limited to 35 V by HP-4192, over a thick cell, results in a weak bias electric field. An additional problem is hardness of antiferroelectric coupling in some materials (e.g. in LC2 and LC3). In our dielectric measurements of the antiferroelectric phase, it is of great importance to apply a bias electric field strong enough to achieve a threshold field

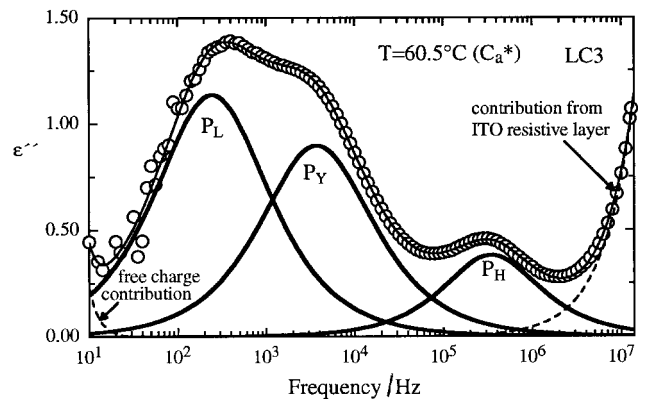


Figure 1. Frequency dependence of the dielectric absorption in the antiferroelectric phase ( $C_a^*$ ) of the single compound LC3. Besides the contributions from dipolar reorientation (thick solid lines), there is a low and a high frequency background (dotted line) from freely moving charges and the ITO conducting layer, respectively. The thin solid line represents the fitting of equation (2) to the experimental results, resulting in the three resolved absorption peaks  $P_L$ ,  $P_Y$  and  $P_H$ .

$E_C$  corresponding to the antiferroelectric–ferroelectric transition. However, applying a bias electric voltage over a thin cell may sometimes cause an electric breakthrough that occurs earlier than the field-induced transition to the ferroelectric state. This led to some limitations on measurements in a bias field, and have barred us, so far, from carrying out measurements close to  $E_C$  in a systematic way.

Another common problem in dielectric measurements is the transport of freely moving charges which results in an additional contribution to  $\epsilon''$  at low frequencies where the measured  $\epsilon''$  increases with decreasing frequency. This low frequency contribution, in some cases, may obscure absorption peaks due to dipolar rotation when located below 100 Hz. At low frequency, the cell impedance increases and may reach a value beyond the capability of the HP-4192 bridge which is limited to

3 M $\Omega$ . This restricts the accuracy of the measurements at lower frequencies. However, if the sample capacitance is large enough, which may be the case when studying high polarization compounds, the accuracy is improved because the impedance becomes measurable by the bridge. It is thus obvious that when investigating antiferroelectric compounds, due to low capacitance, the measurements at low frequency will not be very accurate. An illustrative example of the measured dielectric absorption in an antiferroelectric phase is shown in figure 1. Note that at low frequencies, the measured points are more scattered than at high frequencies. Figure 1 shows that the measured  $\epsilon''$  can be accurately modelled by equation (2), yielding the three peaks shown in the figure. An excellent fit is obtained and a regression coefficient better than 0.999 was obtained throughout.

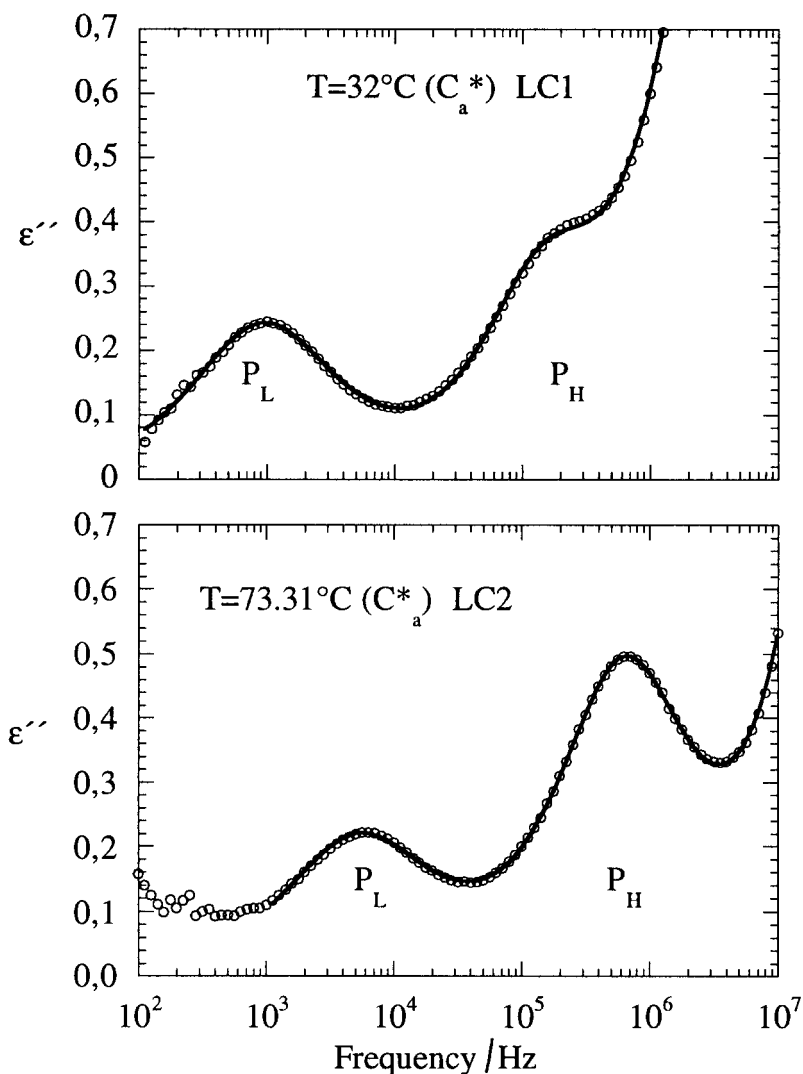


Figure 2. Frequency dependence of the dielectric absorption in the antiferroelectric phases  $C_a^*$  of LC1 and LC2.

#### 4. Results and discussion

This section will be divided into four parts. In the first part, the dielectric spectrum for materials which do not possess a C\* phase and for materials with a C\* phase will be presented, in turn. These results are observed in a measurement geometry where the smectic layers are essentially perpendicular to the cell plates. In the second part, we discuss the dielectric spectrum when the smectic layers were aligned in a direction parallel to the cell plates. We will then be able to compare the spectral results in the planar and quasi-homeotropic orientations. In the third part (§4.3), the effect of a bias electric field on the dielectric spectrum of two materials will be given and we also present the dielectric spectra in the high frequency range (10 MHz to 10 GHz).

##### 4.1. Dielectric spectra from bookshelf samples

With the designation bookshelf, the generic geometry is where the smectic layers are perpendicular, or at least nearly so, to the glass plates. This geometry is relatively easy to obtain by oblique evaporation of SiO on the bounding glass surfaces, eventually assisted by a careful and gentle shearing in a direction perpendicular to the director in the A\* phase. In this phase, and more or less so in the successive lower-temperature phases, the director is perpendicular to the measuring field. As for the number of observed absorptions in the spectrum, different materials show seemingly contrasting behaviour.

##### 4.1.1. Materials which do not exhibit a C\* phase (LC1 and LC2)

If we neglect, for the time being, the non-collective motions around the long axis of the molecules found in the near GHz region (we will return to these in the last section), two excitations are observed in the C<sub>a</sub>\* and C<sub>γ</sub>\* phases (although in the latter case, with only a narrow phase region, the situation is less clear than the former). Figure 2 shows the frequency dependence of the dielectric absorption in the range 10<sup>2</sup> Hz to 10<sup>7</sup> MHz of the mixtures LC1 and LC2 in the antiferroelectric phase. The dielectric spectra contain two absorption peaks P<sub>L</sub> and P<sub>H</sub> separated by almost two frequency decades, in the kHz and MHz range, respectively. In order to extract the values of ε<sub>R</sub> and f<sub>R</sub>, equation (2) has been fitted to the frequency dependent dielectric absorption measured at different temperatures. The dielectric strength and relaxation frequency as a function of temperature, in the different phases of the same materials, are given in figure 3. In the A\* phase the relaxation frequency shows the expected slowing down behaviour with decreasing temperature, and the dielectric strength shows a diverging-like behaviour when approaching the transition A\* to C<sub>α</sub>\* (in the case of LC1) or A\* to C<sub>γ</sub>\* (in the case of LC2). It may be

noted that, while the A\* and C<sub>a</sub>\* phases in LC1 are separated by three intermediate phases (C<sub>α</sub>, C<sub>x</sub>\* and C<sub>γ</sub>\*) only a C<sub>γ</sub>\* phase appears between A\* and C<sub>a</sub>\* in LC2. A detailed discussion of the dielectric behaviour of the C<sub>α</sub> and C<sub>x</sub>\* phases of the LC1 mixture has been published elsewhere [26]. Therefore our discussion will now be focused on the C<sub>γ</sub>\* and C<sub>a</sub>\* phases.

In the ferroelectric phase, the dielectric spectra of LC1 [figure 4(a)] and LC2 [figure 4(b)] show two absorption peaks, separated by three frequency decades. The low and high frequency peaks are centred around 200 Hz and 300 kHz, respectively. The location of these two relaxations is characteristic for the spectrum of the ferroelectric phase. The temperature dependence of ε<sub>R</sub> and f<sub>R</sub> on the high frequency process shows a soft mode-like behaviour in the sense that the dielectric strength ε<sub>H</sub> decreases and the relaxation frequency f<sub>H</sub> increases with decreasing temperature as illustrated in figure 3. The low frequency peak in both materials has the character of a Goldstone mode in the sense that the dielectric strength ε<sub>L</sub> slightly increases and the relaxation frequency f<sub>H</sub> slightly decreases with decreasing temperature. Both modes have, however, a much lower dielectric strength than the corresponding modes belonging to a paraelectric or ferroelectric phase. This is understandable because the ferroelectric phase has a non-zero local polarization, which quenches the soft mode (as is also the case in the normal ferroelectric phase—the ferroelectric is a kind of ferroelectric with low polarization); on the other hand, the lower polarization also diminishes the Goldstone response. At the onset of the antiferroelectric phase, the high frequency peak continues into a corresponding high frequency peak, which lies at practically constant frequency over the whole temperature dependence in LC1, or the frequency of the peak slightly diminishes as in LC2. At the same time, a new Goldstone-like absorption appears as a low frequency peak in both materials. The high frequency mode has actually none of the characteristics of a ferroelectric soft mode, rather the contrary: ε<sub>H</sub> is increasing with decreasing temperature, whereas f<sub>H</sub> is fairly constant (LC1) or decreasing in a non-linear fashion [figure 3, parts (a) and (b), respectively]. It therefore cannot be associated with a soft mode as was done in reference [23]. The low frequency absorption has been attributed by different authors [8, 23–25] to a non-collective reorientation around the short axis. In the later sections, we will present evidence, from dielectric and electro-optic studies explaining why we believe that this assignation is equally inadequate.

In analogy with the C\* phase, the dielectric strength ε<sub>G</sub> and the relaxation frequency f<sub>G</sub> [32] of the ferroelectric Goldstone mode can be written as

$$\varepsilon_G = \frac{1}{2\varepsilon_0 K_\phi q^2} \left( \frac{P}{\theta} \right)^2 \quad (3)$$

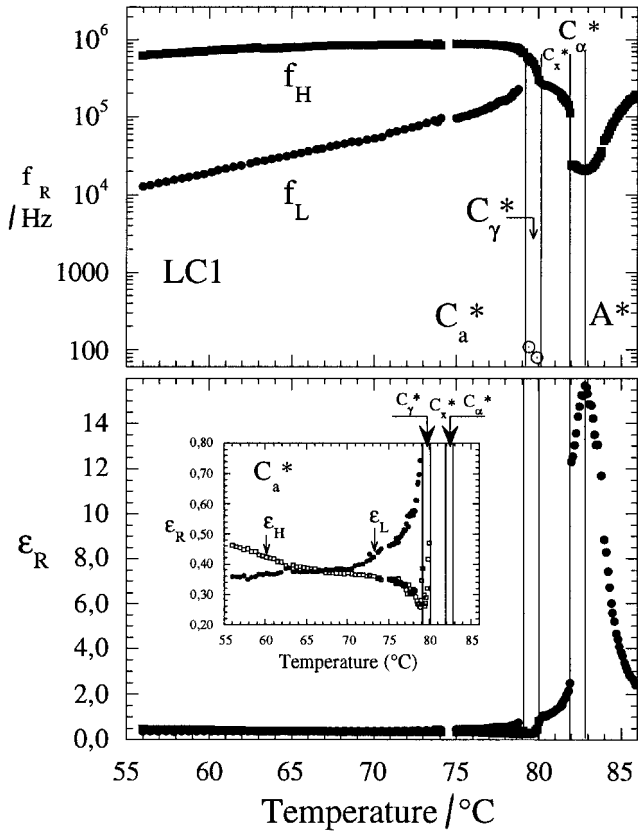


Figure 3(a). Temperature dependence of the relaxation frequencies (upper figure) and dielectric strength (lower figure) measured in the  $A^*$ ,  $C_a^*$ ,  $C_x^*$ ,  $C_\gamma^*$  and  $C_\alpha^*$  phases of LC1. The temperature dependence of the dielectric strengths  $\epsilon_L$  and  $\epsilon_H$  in the antiferroelectric and ferroelectric phases is shown on a larger scale in the inset. There are two modes in the  $C_\gamma^*$  phase, a low frequency mode observed at about 100 Hz and indicated by the two circles in the upper figure, and a high frequency mode in the region  $10^5$  to  $10^6$  Hz.

and

$$f_G = \frac{K_\phi q^2}{2\pi\gamma_\phi} \quad (4)$$

where  $K_\phi$ ,  $\gamma_\phi$ ,  $P$ , and  $\theta$  are the elastic constant for the cone motion, cone mode viscosity, spontaneous polarization and tilt angle, respectively. The length  $q$  is the helical wave vector related to the pitch  $p$  as  $q = 2\pi/p$ . According to one of the proposed models of the  $C_\gamma^*$  phase, the periodic unit consists of three layers, where the tilt in a certain direction in one layer is followed by two layers with tilt direction opposite to that of the first layer. This implies that the effective value of  $P$  in the ferroelectric phase is equal to one-third of the spontaneous polarization in the ferroelectric phase. Thus, from equation (3), it follows that the dielectric strength of the Goldstone mode in the ferroelectric phase

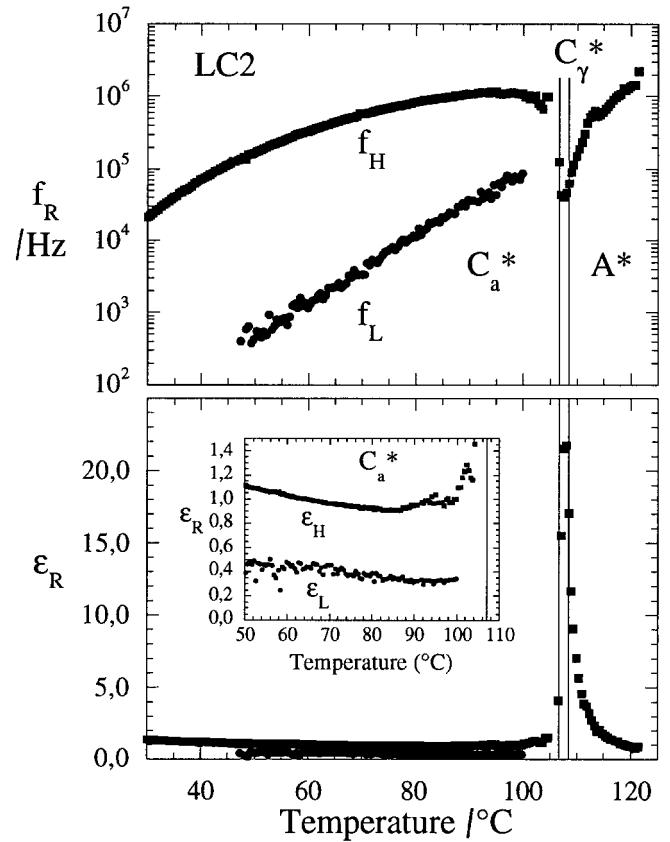


Figure 3(b). Corresponding temperature dependence of the relaxation frequency and dielectric strength in LC2. The dielectric strengths of the  $P_L$  and  $P_H$  processes are likewise plotted on a larger scale.

should be lower than that in the  $C^*$  phase by one order of magnitude if other parameters are unchanged. The helicoidal structure in the ferroelectric phase can be expected to be more rigid than in the  $C^*$  phase, with a correspondingly higher value of  $K_\phi$ . As for the value of  $\epsilon_G$ , this may be compensated for by a longer pitch in the  $C_\gamma^*$  phase. We have measured this pitch [30] and do find that it shows a tendency towards a diverging-like behaviour in the narrow  $C_\gamma^*$  phase. However, this can only be seen if the measurements are performed on free-standing films; the behaviour in all other cases shows only a small discontinuity and a pitch value deviating less than about 20% from the value in the adjacent  $C_a^*$  phase (or  $C^*$  phase, in the case that both phases are present). Hence it seems to be difficult in practice to realize the true pitch value in the  $C_\gamma^*$  phase corresponding to thermodynamic equilibrium, despite the short pitch (for any of the investigated materials it does not exceed  $0.8\ \mu\text{m}$ ) combined with a thick (18 or  $36\ \mu\text{m}$ ) cell. This can be expected, due to the smearing-out and surface hysteresis effect from the boundary surfaces, but also

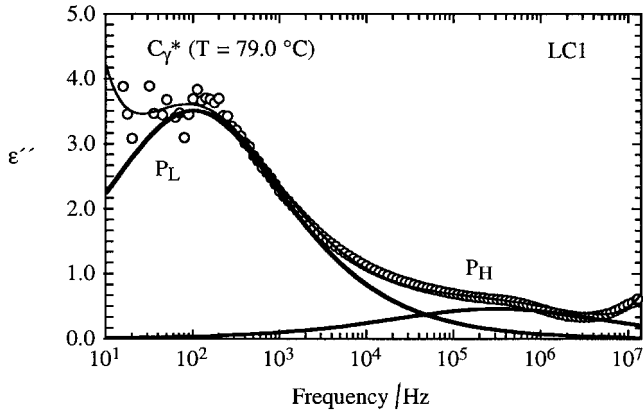


Figure 4(a). Frequency dependence of the dielectric absorption in the ferroelectric phase of LC1; two peaks have been resolved and denoted  $P_L$  and  $P_H$ . The thin solid line represents the fitting of equation (2) with two Cole–Cole functions; the thick solid lines are the extracted absorption peaks from the fitting. The  $P_H$  peak is very broad and not very well resolved due to the dominating low frequency contribution, as well as the high frequency background caused by the ITO resistive layer.

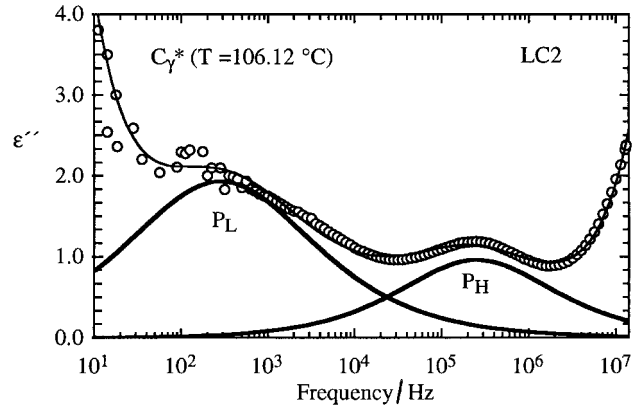


Figure 4(b). Frequency dependence of the dielectric absorption in the ferroelectric phase of LC2.

from the fact that we have coexisting phases. We will return to this last effect in more detail below.

Summarizing the empirical results for materials lacking the  $C^*$  phase, we may state the following. In the ferroelectric  $C_\gamma^*$  phase we have an active Goldstone mode (typically around 200 Hz) and a soft-like mode (typically around 300 kHz). Both are weak, as can be expected, and it is difficult to say anything about the true nature of these modes solely from the very limited amount of information that can be extracted out of the narrow  $C_\gamma^*$  phase range. At the onset of the  $C_a^*$  phase, the Goldstone mode vanishes whereas the soft mode transforms, or is replaced by two new modes ( $P_L$  and  $P_H$ ) in the low MHz region. Both seem to be collective excitations. While it cannot be excluded that the low frequency mode is of Goldstone type, the high frequency mode is definitely not of soft mode type.

#### 4.1.2. Materials with a $C^*$ phase (LC3 and LC4)

In the single compounds LC3 and LC4, characterized by the phase sequence  $C^* - C_\gamma^* - C_a^*$  with descending temperature, it is easy to localize the two absorptions  $P_L$  and  $P_H$  in the  $C_a^*$  phase, corresponding to the same modes in the  $C_a^*$  phase of the previous materials (figures 1 and 5). But in addition to this, we have in each case a new strong absorption slightly above 1 kHz. In LC3 this mode is intermediate in frequency ( $\sim 4$  kHz) between  $P_L$  and  $P_H$ , while it is situated ( $\sim 1$  kHz) below both of them in LC4. It is easy to identify the nature of this mode if we follow the evolution of the dielectric spectrum with temperature through the different phases of the material. This is illustrated in figure 6 for the case of

LC3. The powerful Goldstone mode in this material is located at about 10 kHz, and is practically independent of temperature across the  $25^\circ C^*$  range and even through the  $8^\circ C_\gamma^*$  range, and persists to a surprising degree deep down into the  $C_a^*$ . According to the dielectric properties, there does not even seem to be a phase change at  $92^\circ C$  between  $C_a^*$  and  $C_\gamma^*$ , yet this is a first order transition. The characteristic features of the dielectric spectrum of the ferroelectric phase, which we could study in the previous materials (a weaker absorption at lower frequency), are now completely hidden by the powerful  $C^*$  phase absorption. The strength of this absorption falls off on entering the  $C_a^*$  phase (figure 7) but can be traced, slightly downshifted in frequency, even to the lowest temperature region of the  $C_a^*$  phase ( $55^\circ C$ , lowest part of figure 6).

In the single compound LC4 in which the ferro- and ferroelectric phases appear in narrower temperature intervals ( $10^\circ$  and  $2^\circ$ , respectively) the situation is only

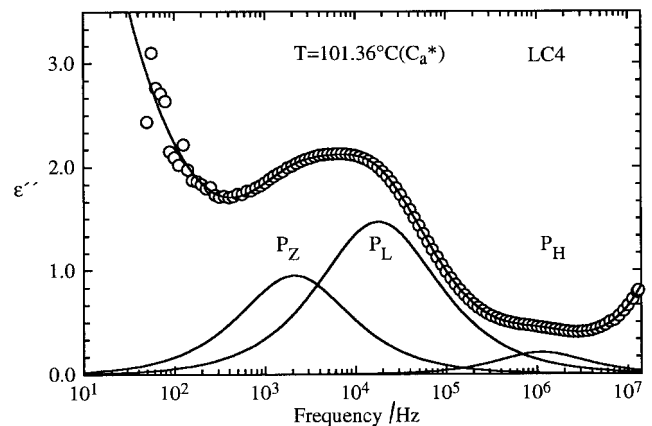


Figure 5. Frequency dependence of the dielectric absorption in the antiferroelectric phase ( $C_a^*$ ) of the single compound LC4.



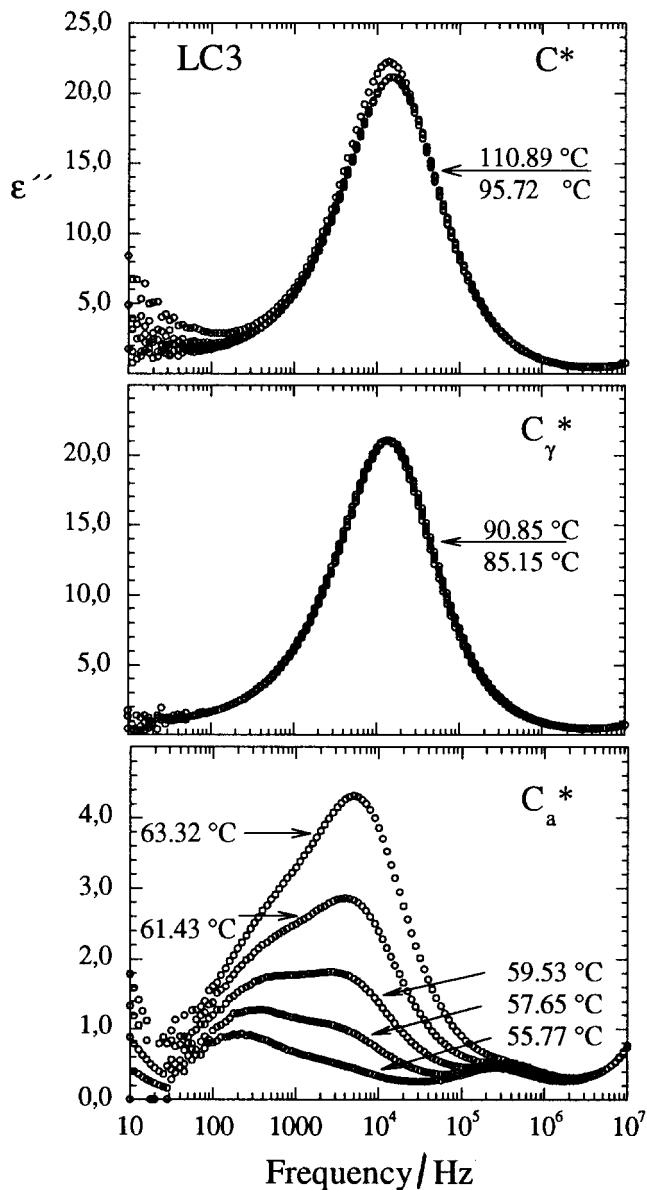


Figure 6. Evolution of the dielectric spectrum with temperature in the ferroelectric, ferrielectric and antiferroelectric phases of LC3. The absorption peak in the  $C^*$  phase is due to the ferroelectric Goldstone mode. The absorption peak in the  $C_\gamma^*$  phase has almost the same amplitude and the same frequency location, and both features are also essentially independent of temperature. In the  $C_a^*$  (lower figure), the same peak can be localized as the peak in the middle of the spectrum: its amplitude has now decreased to 20% and its location has been slightly shifted with temperature.

slightly different. Here the strength of the Goldstone mode decreases rapidly in the  $C^*$  phase (figure 9), [corresponding to the first rapid decrease below the  $A^* \rightarrow C^*$  transition, figure 7] and even more rapidly in the  $C_\gamma^*$  phase (figure 9) and the middle part of figure 8. This allows us to observe the  $P_L$  and  $P_H$  absorptions

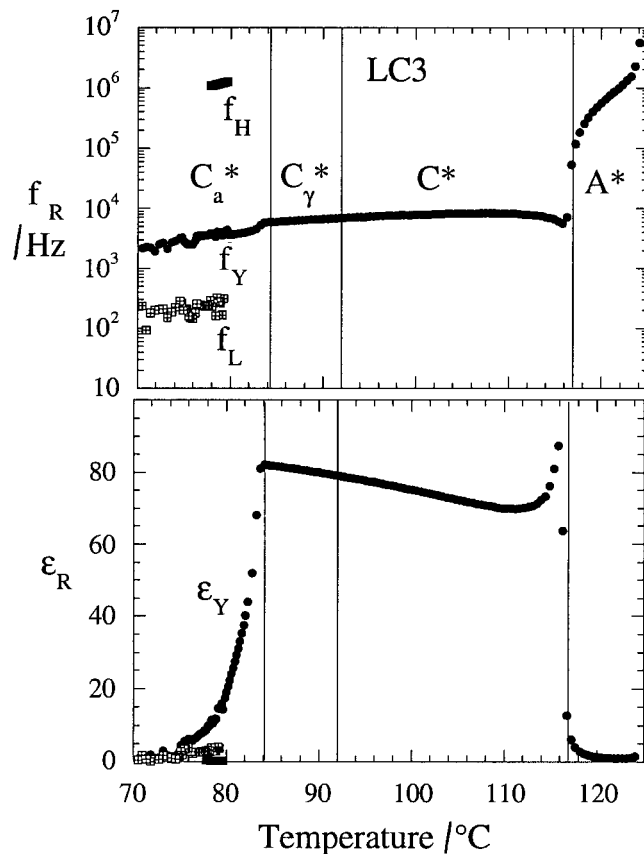


Figure 7. Temperature dependence of the relaxation frequency and dielectric strength in the different phases of LC3. Note that the three branches ( $f_H$ ,  $f_Y$ ,  $f_L$ ) in the  $C_a^*$  phase could not be resolved at the onset of that phase due to the dominant contribution of the  $C^*$  Goldstone mode.

even in the  $C_\gamma^*$  phase, before entering  $C_a^*$ . The abrupt drop in both frequency and dielectric strength to the new values of  $f_Z$ ,  $\epsilon_Z$  (figure 9) further indicates that this signal comes from the  $C_\gamma^*$  phase in LC4. It is thus the Goldstone mode of the ferrielectric phase which penetrates into the antiferroelectric phase in this case, while the Goldstone mode at least penetrates into the  $C_\gamma^*$  phase.

#### 4.1.3. Hereditary peaks

The experimental data from materials with a  $C^*$  phase are, taken together, quite conclusive. Both of the transitions  $C_a^* \rightarrow C_\gamma^*$  and  $C_\gamma^* \rightarrow C^*$  are first order. In the antiferroelectric phase, as well as in the ferrielectric phase, only two characteristic absorptions exist (here denominated  $P_L$  and  $P_H$ , although their origin might be quite different in the two phases—this is discussed in the next section). The additional peak found in each of these phases, in the case of LC3 (where the  $C^* \rightarrow C_\gamma^*$  transition does not seem to occur while recording the

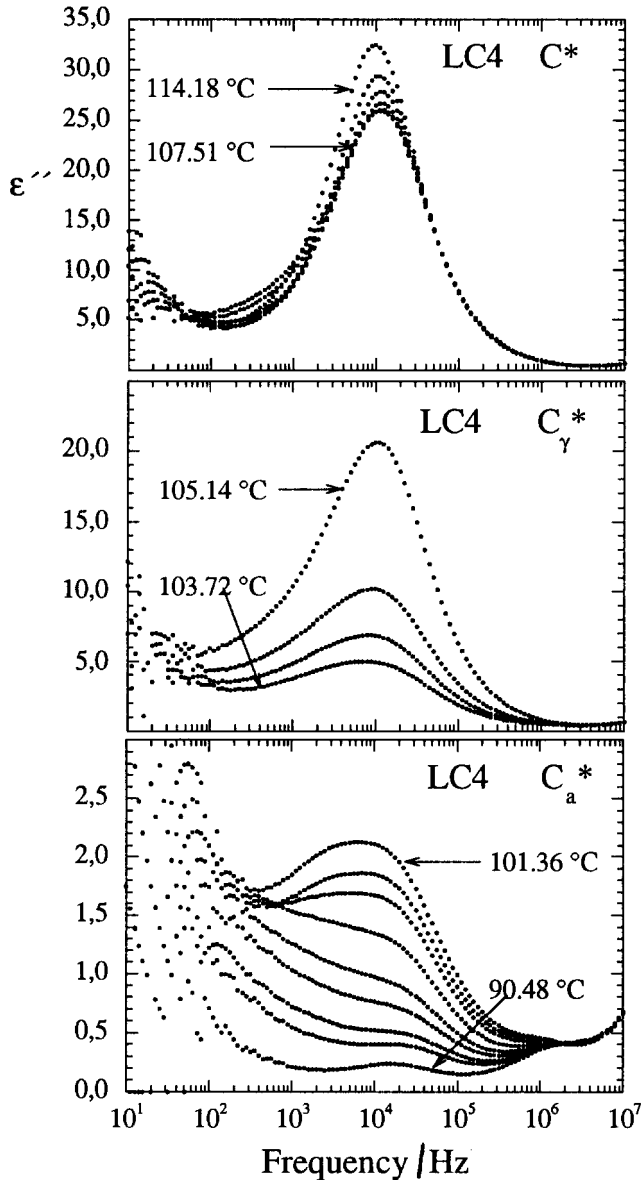


Figure 8. Evolution of the dielectric spectrum with temperature in the ferroelectric (upper figure), ferrielectric (middle figure) and antiferroelectric (lower figure) phases.

spectrum) is clearly nothing else than the Goldstone mode pertaining to the  $C^*$  phase appearing over a much larger temperature interval than that corresponding to the quoted phase sequence. We might call such peaks, which are not spurious but real, but not characteristic for the phase in question, *hereditary peaks*. The reason for the appearance of such peaks is the coexistence of phases bounded by first order transitions. This would also explain some of the results published in the literature [27]. In the present case it is easy to check by microscopy that the (high birefringence)  $C^*$  phase coexists with the  $C_\gamma^*$  and with the  $C_a^*$  phase down to low

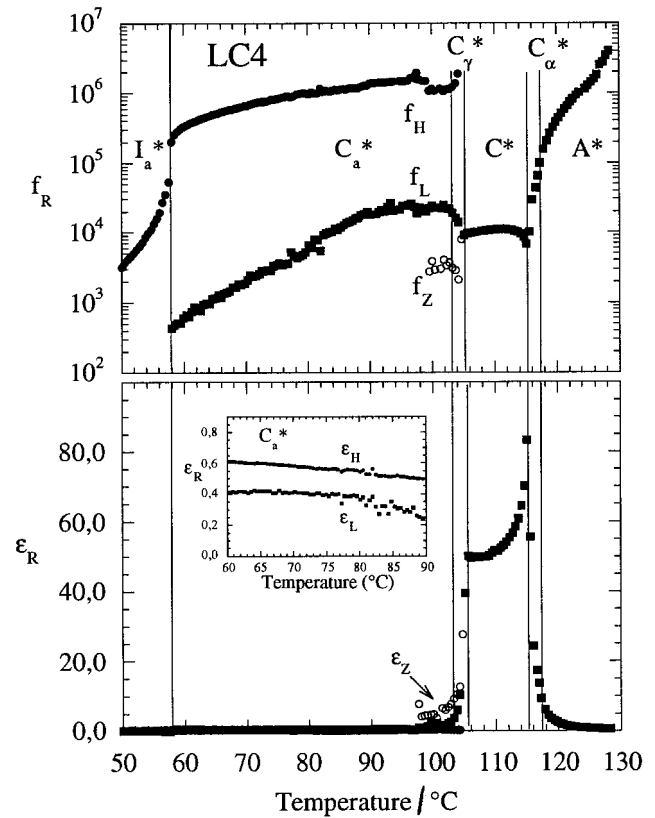


Figure 9. Temperature dependence of the relaxation frequency (upper figure) and dielectric strength (lower figure) in the different phases of LC4. One of the remarkable features in this figure is the sharp decrease of the dielectric strength of the Goldstone mode in the  $C^*$  phase with decreasing temperature (lower figure) and its even sharper decrease in the  $C_\gamma^*$  phase. The absorption ( $\epsilon_Z$ ,  $f_Z$ ) found in the lower phases is evidently the surviving Goldstone mode from the  $C_\gamma^*$  phase.

temperatures. As can be expected, the persistence of the  $C^*$  phase is stronger the more stable it is thermodynamically; this effect is more pronounced in LC3 than in LC4. In the case of LC4 where the transition  $C^* \rightarrow C_\gamma^*$  can be seen, we identify the low frequency mode  $f_L$ , the high frequency mode  $f_H$  and the third relaxation  $f_Z$  as seemingly splitting from the Goldstone mode  $f_G$  in the  $C^*$  phase. [If one disregards the relaxation  $f_Z$ , the situation is very similar to that in figure 3(a) for LC1.] It is clear that the narrow  $C_\gamma^*$  phase coexists as well with the  $C^*$  phase in its upper region, as with the  $C_a^*$  phase in its lower region and, in fact, a hereditary peak may come from both directions into the  $C_\gamma^*$  phase, even if supercooling always dominates over superheating. Our interpretation of the origin of the additional peaks ( $P_Y$ ,  $P_Z$  in LC3 and LC4) means that the temperature interval over which the peaks are resolvable actually represents a two-phase region. It is easily conceivable that the ever present  $C^*$  phase fluctuations

(Goldstone mode) in the lower-lying phases could be interpreted as dielectric effects in a one phase region. However, such fluctuations are also present in the LC1 and LC2 materials, where no such effects have been found.

#### 4.1.4. The characteristic relaxations in the $C_a^*$ phase

As we have pointed out previously, the molecular aspects of the  $P_L$  and  $P_H$  processes, as can be seen from the literature, are a subject of controversy [8, 16–28]. We would like to summarize comment on these interpretations in the light of our results so far, before presenting new arguments.

*The  $P_L$  process:* In all of our materials studied, the relaxation frequency of the  $P_L$  process decreases with decreasing temperature. A similar temperature dependence has been reported for other materials. The dielectric strength does not show a coherent trend:  $\varepsilon_L$  of LC2–LC4 shows a slight increase on cooling, whereas it varies in an opposite fashion in the case of LC1. Many authors [8, 23–25] have attributed the  $P_L$  process to a reorientation around the molecular short axis. Since this interpretation has become common in the literature, we have to discuss it in some detail. As this molecular process is ideally observed in quasi-homeotropic samples, we will present the discussion separately in the next section.

*The  $P_H$  process:* This process has often been associated with a soft mode, as proposed for instance in [23]. If we look at the results on LC2 [figure 3(b)] we note that just below the  $C_\gamma^* - C_a^*$  transition,  $f_H$  is rising and  $\varepsilon_H$  decreasing in a way which may remind one of a soft mode. This behaviour is, however, limited to a short temperature region after which  $f_H$  may decrease by several decades, a feature which has been described by several authors [23, 24]. Qualitatively, one might argue for such a possible temperature dependence in the following way: the relaxation frequency  $f_H$ , within a large range of validity, can be written as

$$f_H \sim \frac{K_S}{\gamma_S} \quad (5)$$

where  $K_S$  and  $\gamma_S$  are the elastic constant and rotational viscosity of the soft mode. These two coefficients have different functional dependence on temperature. The coefficient  $K_S$  should be proportional to  $\theta^2$  and  $\gamma_S$  should follow an Arrhenius law, thus

$$f_H \sim \frac{\theta^2}{\gamma_0 \exp\left(\frac{E_a}{K_B T}\right)}. \quad (6)$$

However, at lower temperatures in the  $C_a^*$  phase, the tilt angle becomes almost temperature independent and

therefore the relaxation frequency would start decreasing, according to

$$f_H \sim \exp\left(-\frac{E_a}{K_B T}\right). \quad (7)$$

Another aspect which might associate  $P_H$  with a soft mode is that the values of the relaxation frequency are high and comparable with those for the soft mode in the  $A^*$  phase [figure 3(b)]. On the other hand, it is also often observed that  $\varepsilon_H$  increases and  $f_H$  decreases, or is constant after the onset of the  $C_a^*$  phase, [cf. for instance figures 9 and 3(a)], a tendency that can hardly be explained on the basis of a soft mode model. All these arguments give only vague support in either direction; on the other hand the soft mode interpretation cannot be ruled out completely on the basis of these data. In order to decide the question, we have therefore performed measurements of the spectra in the presence of a bias field, to be presented in §4.3.

#### 4.2. Dielectric spectra from quasi-homeotropic samples

The molecular reorientation around the short axis is one of the most extensively studied molecular processes in liquid crystal dielectric spectroscopy [32]. This process is characterized by a single relaxation mechanism, and its characteristic frequency varies from the high MHz region, in nematics, to the low MHz and kHz regimes in smectics. In highly ordered smectics, the process is normally shifted down even below the kHz range of the spectrum. The best way to probe the reorientation around the molecular short axis is to prepare a smectic  $A^*$  sample in the homeotropic orientation (layers parallel to the glass plates). After cooling to tilted smectics, the director then makes an angle  $\theta$  (tilt angle) with the measuring electric field. Also in this case the measurement geometry (called quasi-homeotropic) allows us to probe the flipping motion around the short axis, although the dielectric strength  $\varepsilon_{\text{hom}}$  of this process is lower than that in the  $A^*$  phase. In the quasi-homeotropic orientation,  $\varepsilon_{\text{hom}}$  is related to the dielectric permittivity component parallel to the director  $\varepsilon_{\parallel}$  by the relation

$$\varepsilon_{\text{hom}} = \varepsilon_{\parallel} \cos^2 \theta. \quad (8)$$

In fact, this molecular process can also be probed in the bookshelf geometry of tilted smectics where the dielectric strength  $\varepsilon_p$  (p stands for planar) will be lower than  $\varepsilon_{\text{hom}}$ . However, the relaxation frequencies  $f_p$  and  $f_{\text{hom}}$  are identical. In the case of thick samples of helicoidal tilted smectics, with the helix axis parallel to the glass plates,  $\varepsilon_p$  is given by

$$\varepsilon_p = \frac{1}{2} \varepsilon_{\parallel} \sin^2 \theta. \quad (9)$$

As seen from equation (9), if we have an ideal bookshelf

geometry of a non-tilted smectic, the contribution in the field direction of the flipping motion around the short axis equals zero. In tilted smectics, if the tilt plane is parallel to the glass plates, it will effectively give the same result as that in the orthogonal smectics. Thus, in tilted smectics, it is the swinging out of the director from the plane of the glass plates (as in the case of a helicoidal structure) which enables us to probe this process. If we compare the dielectric strength from the molecular rotation around the short axis in the two measuring geometries, equations (8) and (9) give the ratio

$$\frac{\varepsilon_p}{\varepsilon_{\text{hom}}} = \frac{1}{2} \tan^2 \theta \quad (10)$$

which is always a small number  $\ll 1$ . Deep in the  $C_a^*$  phase, where the tilt angle reaches a saturation value and becomes temperature independent, it will reach its maximum value. For a typical saturation value of  $25^\circ$ ,  $\varepsilon_p/\varepsilon_{\text{hom}}$  will be about 0.1.

We may summarize the situation in the following way. In the homeotropic or quasi-homeotropic geometry (smectic layers parallel to the glass plates), we always detect the signal from the molecular motion around the short axis. Moreover, this signal should be detected in all liquid crystal phases that occur for the substance, unperturbed by the transitions between them. In the planar or bookshelf geometry (director essentially parallel and smectic layers essentially perpendicular to the glass plates) we *may* be able to detect a signal from the same process in the tilted smectic phases, and hence in the antiferroelectric phase. However, an observed peak may only be attributed to this process provided that the three following criteria are fulfilled. (1) The relaxation frequency of this process must coincide with that observed in the quasi-homeotropic orientation. (2) The temperature dependence of this process (its activation energy) should be the same as that observed in the quasi-homeotropic orientation. (3) The dielectric strength of the process in question must increase with increasing tilt, i.e. the dielectric strength should increase with decreasing temperature. The highest permissible value for the ratio  $\varepsilon_p/\varepsilon_{\text{hom}}$  should be of the order of 0.1. Violation of any of these conditions is sufficient to rule out the molecular motion around the short axis as being involved in the process.

We may now turn to the experimental situation. Figure 10 shows the relaxation frequency  $f_L$  of the low frequency peak ( $P_L$ ) observed in LC1, as a function of temperature. It is compared with the relaxation frequency for the reorientation around the short axis,  $f_{\text{hom}}$ ; the corresponding dielectric strengths are also shown. As expected,  $f_{\text{hom}}$  and  $\varepsilon_{\text{hom}}$  vary in a perfectly continuous fashion through all the phases  $C_a^*$ ,  $C_\gamma^*$ ,  $C_x^*$ ,  $C_\alpha^*$  and  $A^*$ .

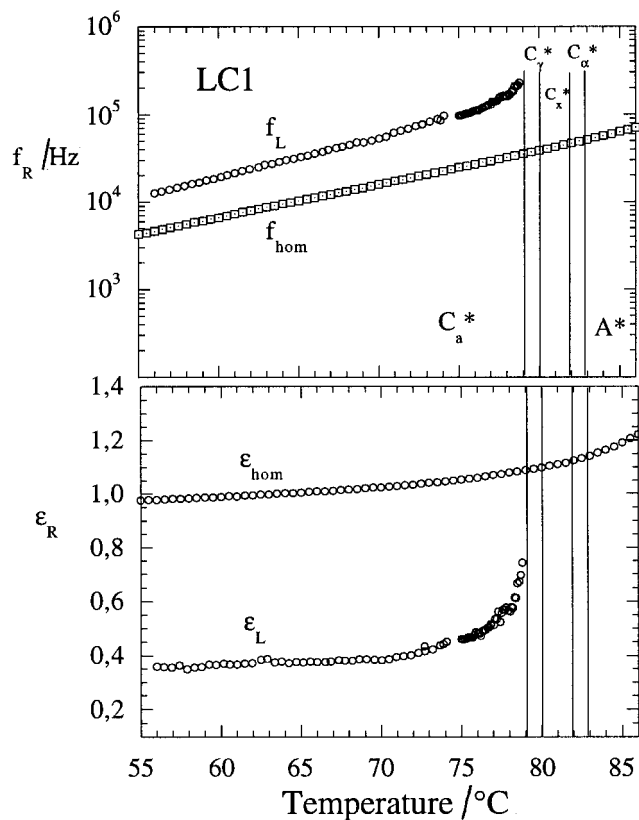


Figure 10. Temperature dependence of the relaxation frequency and dielectric strength for the low frequency peak detected in the planar (bookshelf) configuration of LC1, compared with the corresponding parameters due to the molecular reorientation around the short axis ( $f_{\text{hom}}$ ,  $\varepsilon_{\text{hom}}$ ), detected in the homeotropic configuration of the same sample.

It is true that  $f_L$  (which is the  $f_p$  above in our general discussion) shows the same, or almost the same activation energy as  $f_{\text{hom}}$ , but other criteria, (1) and (3), are violated. First,  $f_L$  lies about a factor of two higher than  $f_{\text{hom}}$ . Moreover,  $\varepsilon_L$  does not increase with decreasing temperature and the value  $\varepsilon_L/\varepsilon_{\text{hom}}$  is about 0.4 in the lower range and even 0.7 in the high temperature range of the  $C_a^*$  phase, and thus more than five times the permissible value. The low frequency absorption detected in the antiferroelectric phase of LC1 therefore stems from a different process than the reorientation around the molecular short axis.

The situation is slightly more complicated in the single compounds. As shown in figure 11, both the value of the relaxation frequency and the activation energy are so similar that they could easily be confused. But  $\varepsilon_L$  decreases instead of increasing when the tilt increases, and  $\varepsilon_L/\varepsilon_{\text{hom}}$  is certainly larger than the permissible value. At high temperatures,  $\varepsilon_L$  even becomes larger than  $\varepsilon_{\text{hom}}$ . Furthermore, the signal does not penetrate into the  $C^*$  phase. A different experiment has been carried out on

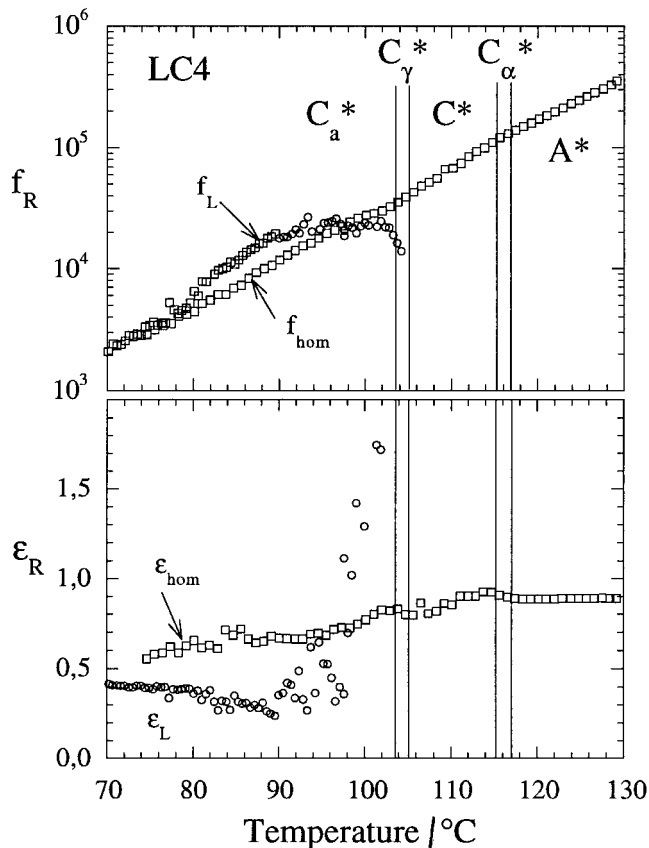


Figure 11. The same measurements as in figure 10, performed on LC4.

LC3. Figure 12 shows the dielectric absorption in two different geometries, planar/homeotropic, detected on the same sample at the same temperature (55°C). The first spectrum (planar) contains the dominating hereditary peak from the C\* phase between the P<sub>L</sub> and P<sub>H</sub> absorp-

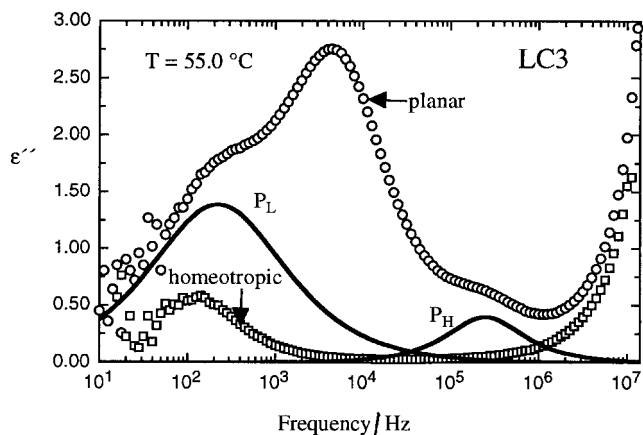


Figure 12. Frequency dependence of the dielectric absorption in the C<sub>a</sub>\* phase measured for the planar (circles) and homeotropic (squares) orientation of the same sample of LC3, at a fixed temperature in the low temperature end of the phase.

tions. By applying a strong shear to the cell (at the same temperature), an excellent quasi-homeotropic orientation was obtained. This allows us to perform a second measurement, *on the same cell*, but now in the homeotropic orientation. In this geometry we detect only the peak due to the reorientation around the short axis. We see that the P<sub>L</sub> absorption lies at practically the same frequency. It is therefore understandable that P<sub>L</sub> may sometimes be mistaken as being due to this non-collective process. However, the ratio  $\epsilon_L/\epsilon_{\text{hom}}$  is larger than the permissible value by at least a factor of 3.

#### 4.3. Dielectric spectra in the presence of a bias electric field

Dielectric measurements in the presence of a bias electric field constitute one of the crucial tests which may provide decisive results in determining the molecular origin of different absorption peaks in the dielectric spectrum. Experimentally, a bias electric field strongly affects the dielectric spectrum of helicoidal ferroelectric and antiferroelectric phases. The effect on the dielectric strength  $\epsilon_G$  and relaxation frequency  $f_G$  of the Goldstone mode in the C\* phase has been studied by many authors [12, 33]. The effect of a bias field in ferroelectric and antiferroelectric phases has also been investigated [23–28, 34]. In the C\* phase, the Goldstone mode dielectric strength usually decreases strongly with increasing bias field and above a certain critical field  $E_C$ ,  $\epsilon_G$  decreases abruptly towards zero. This critical field corresponds to the helix unwinding by which means all dipoles are aligned in the field direction. We have earlier [26] been able to describe in detail how the dielectric spectrum of the antiferroelectric phase evolves in the presence of a bias electric field and will only remind readers here of the most important observations. The remarkable feature is that both absorption peaks (P<sub>L</sub> and P<sub>H</sub>) first *sharpen* (without appreciable change in position) with a corresponding increase in the dielectric strengths  $\epsilon_L$  and  $\epsilon_H$ . When the bias field reaches the threshold value for the antiferroelectric–ferroelectric transition the P<sub>H</sub> peak vanishes completely (figure 13). Hence this peak is related to the antiferroelectric order and the process is of a collective nature. We have argued [26] that this is a fluctuation in the anti-tilt pairs where adjacent molecules move in opposite phase. The dielectric strength of the low frequency peak also falls off abruptly at the transition, but not to zero. It persists in the ferroelectric state with a low value of  $\epsilon_L$  and with a relaxation frequency of about half the previous value. This means that P<sub>L</sub> is related to a collective mode which is independent, except for the absolute value of  $\epsilon_L$  and  $f_L$ , of whether the molecules move as anti-tilt pairs or as single molecules in unison. Strong arguments were further given as to why none of the peaks P<sub>L</sub> and P<sub>H</sub> could have anything to do with

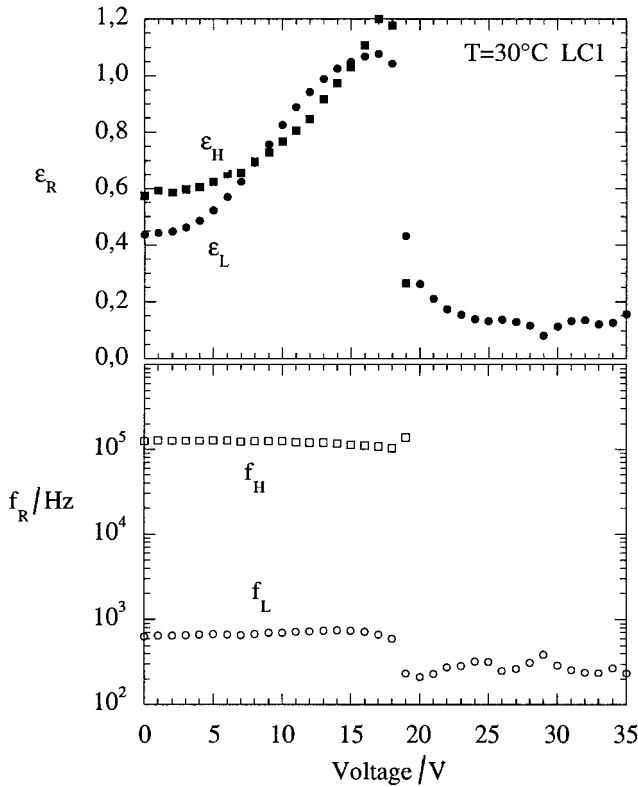


Figure 13. Bias field dependence of the dielectric strength (upper figure) and relaxation frequency (lower figure) in the  $C_a^*$  phase. The threshold field for the antiferroelectric to ferroelectric transition is about  $9 \text{ V } \mu\text{m}^{-1}$ .

fluctuations in  $\theta$  (soft mode), i.e. with the collective process corresponding to reorientation around the short axis. The discussions in the previous sections have indicated that  $P_L$  has features typical of a Goldstone mode. If the molecules in adjacent layers of the  $C_a^*$  phase have tilts which are not quite in opposite directions, but offset by a small angle, there is a local polarization which is macroscopically cancelled only by the helicoidal superstructure. This kind of antiferroelectric order would have Goldstone-like excitations, though with a low value of the dielectric strength. After the field-induced transition to the ferroelectric state the excitations will not be the typically very strong ones characteristic of a ferroelectric phase, because the ferroelectric state is only the antiferroelectric phase in the presence of a strong electric field. Thus, the field will quench the fluctuations and we will dielectrically measure only a small strength. All features of the picture presented so far will finally be supported by the results of the electro-optic measurements, to be described in the next section.

#### 4.4. Non-collective excitations studied at high frequencies

The non-collective or molecular excitations are reorientations around the short axis and those around

the long axis (including internal rotations by parts of the molecules relative to other parts). The former, with characteristic frequencies typically from 1 kHz ( $C_a^*$  phase) to 100 kHz ( $A^*$  phase) were studied in §4.2 (homeotropic samples). The dynamics of motions around the long axis are such that we have to go three orders of magnitude higher in order to study them. The experiments further have to be performed in the planar (bookshelf) configuration. Such measurements on the frequency dependence of the dielectric absorption in the  $A^*$  and  $C_a^*$  phases of LC1 are shown in figure 14(a). By fitting Cole-Cole functions to these curves, the relaxation frequency, dielectric strength and distribution parameter have been determined at different temperatures. From the measurement geometry, the value of the relaxation frequency, the activation energy and the distribution parameter, it can be concluded that these absorption peaks are connected with the molecular reorientation around the long axis. The distribution

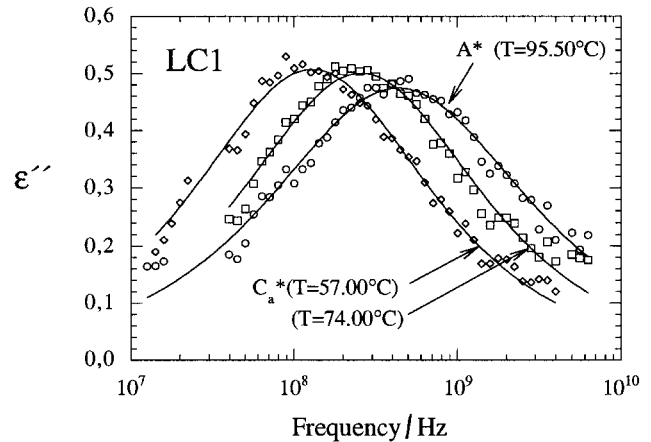


Figure 14(a). The high frequency dielectric spectrum in the  $A^*$  and  $C_a^*$  phases of LC1.

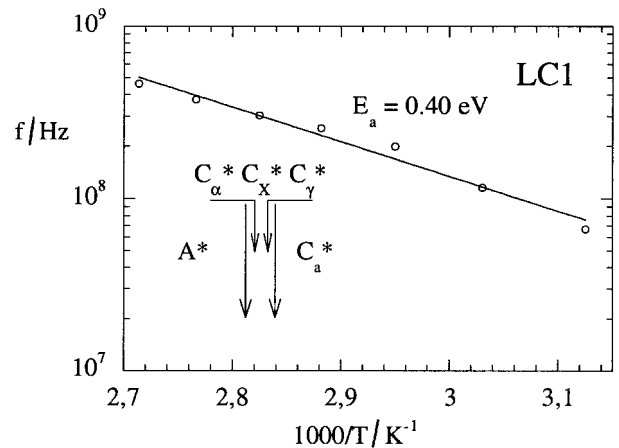


Figure 14(b). Arrhenius plot of the high frequency process: the fast reorientation around the molecular long axis.

parameter is found to be relatively large: its average value equals 0.35. We may conclude from this result that different processes are involved. This is not surprising: first of all, LC1 is a multicomponent mixture which implies that different molecules have slightly different characteristic frequencies. This is, however, not the only reason for the broad distribution, because it is also found that single component systems exhibit a large value of the distribution parameter [35]. In addition to the rotation of the molecule as a whole, other contributing processes could be the independent reorientation of the alkyl groups and other reorientations around single bonds and general small angle reorientations of permanent dipole moment components around the director. The relaxation frequency found for the molecular rotation around the long axis in different phases of LC1 has been plotted against  $1/T$  in figure 14(b). As can be seen from the figure,  $f_R$  does not show any remarkable changes at the different phase transitions. The activation energy  $E_a$ , found to be equal to 0.40 eV, is to be considered as an average for the involved motions, which we can not differentiate. These measurements have been made by time domain spectroscopy; this value is comparable with the reported results in the literature for different systems [36].

### 5. Detection of electro-optically active processes

Collective fluctuations that have been detected by dielectric measurements exhibit an electro-optic response. Thus, it is possible further to confirm our interpretation of the collective aspect of the  $P_L$  and  $P_H$  processes by means of electro-optic studies. In the present work, a comparative study of the electro-optic and dielectric measurements has been carried out on the LC1 material. If a d.c. electric field is applied to an antiferroelectric liquid crystal aligned in the bookshelf geometry, a linear electro-optic response is found, corresponding to the linear part in the  $P$ - $E$  hysteresis curve [figure 15(a)]. The effect is similar to the electroclinic effect in the paraelectric phase, and the linear increase in optical transmission can be interpreted as a linear tilt of the optic axis, at least for  $E \ll E_C$ , the antiferroelectric-ferroelectric transition. So far this linear effect has been regarded as a nuisance, because it diminishes the quality of dark state in AFLC displays. However, at the same time, it is one of the most powerful of the linear electro-optic effects which is at our disposal in liquid crystals. It is not quite as fast as the electroclinic effect in the  $A^*$  phase, but has, in return, a higher power of modulation. In reference [26] we were able by dielectric spectroscopy to identify the molecular motion responsible for this linear process, and to relate it to the  $P_H$  relaxation in the spectrum. This is the already mentioned anti-phase cone motion, illustrated in figure 15(b). We will here be able

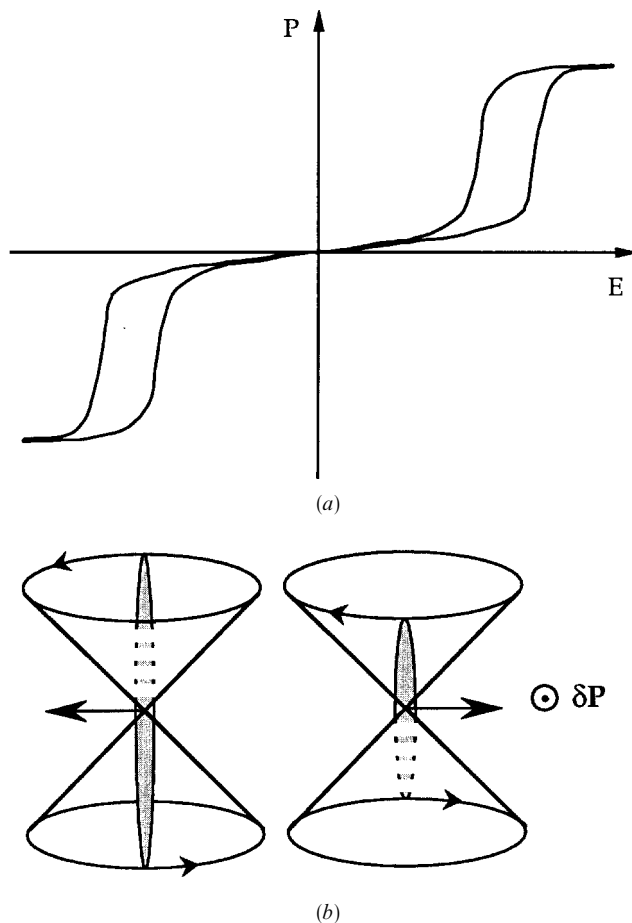


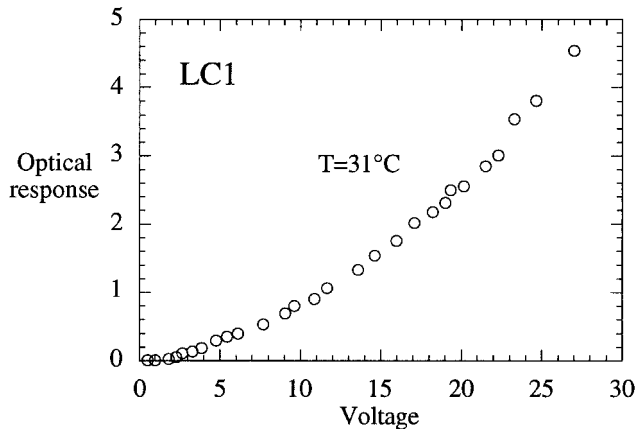
Figure 15. (a) Hysteresis curve for an antiferroelectric liquid crystal (quantitatively) showing the initial linear increase in polarization with applied electric field; (b) the corresponding anti-phase cone motion at the beginning phase of unwinding.

to strengthen the previous conclusion by electro-optic studies.

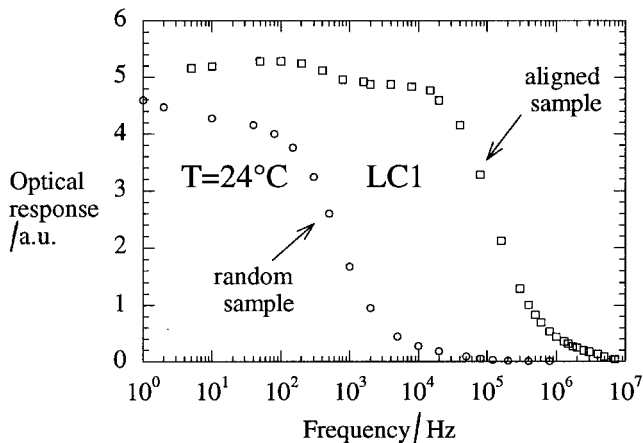
If we apply a sine-shaped voltage to a well-aligned bookshelf sample between crossed polarizers (parallel and perpendicular to the smectic layers) we find a very characteristic optical response in the  $C_a^*$  phase [figure 16(a)]. The optical transmission increases linearly from the initial dark state when the voltage is increased. In contrast to the electroclinic response, however, this response does not, at first, show a tendency to saturation when we further increase the voltage, but rather deviates in the opposite fashion. Thus, electro-optically we already have a strong indication that we are not exciting a soft mode. The linear modulation around the dark state follows the sinusoidal variation of the applied field faithfully up to quite high frequencies. The response time is about  $10 \mu\text{s}$  in this material (Chisso CS-4000). It is independent of the applied electric field, which is another feature making the effect very similar

to the electroclinic (soft mode) response. Increasing the electric field thus only increases the amplitude of the modulation.

In figure 16(b) we show the variation of the optical signal ('aligned sample') when the frequency is subjected to variation while keeping the amplitude of the applied electric field at a fixed value (1.5 V across the 2- $\mu\text{m}$ -thick



(a)



(b)

Figure 16. (a) The linear electro-optic effect: optical transmission from the initially dark field-free state as a function of applied voltage. Data on Chisso CS-4000 (LC1) taken at 30°C with the applied field being a 120 Hz sine wave; (b) frequency dependence of the optical response shown in (a)—'oriented sample'. This response is connected with the field induced changes in the optic axis. The cut-off frequency is at 100 kHz; the dielectric relaxation peak at high frequency ( $P_H$ ) coincides with this electro-optic cut-off. It may be noted that very close to 10 MHz, the optical response exhibits a further drop which is attributed to the cell cut-off. In the diagram are also shown the results for the second, quadratic electro-optic effect—'random sample'—of LC1. Here the optical response is attributed to the changes in effective birefringence with electric field. The cut-off at 1 kHz coincides with the dielectric relaxation peak ( $P_L$ ) at low frequency characteristic of the  $C_a^*$  phase.

sample). We see that the process has a cut-off frequency at about 100 kHz. This coincides with the relaxation frequency of the  $P_H$  process found from dielectric spectroscopy for the same material, at the same temperature (30°C).

Any other electro-optic effect present in this linear regime ( $P-E$ ) of the  $C_a^*$  phase will evidently be obscured by the strong response just described. It is, however, possible to extract a second effect in the presence of the first one in the following way. Instead of working with a homogeneously aligned sample, we make the local direction of the layers as random as possible over the sample surface. This measurement geometry has been achieved by cooling the sample rapidly from the isotropic phase. The sample is still between crossed polarizers, but the angle  $\psi$  between the projection of the director on the glass plates and the transmission direction of the polarizer randomly varies over the sample plane ( $x, y$ ). The intensity of the transmitted light therefore varies as

$$I(x, y) = I_0 \sin^2 2\psi(x, y) \sin^2 \delta/2 \quad (11)$$

where

$$\delta = \frac{2\pi d}{\lambda} \Delta n_{\text{eff}} \quad (12)$$

and

$$\Delta n_{\text{eff}} = \frac{n_o n_e}{(n_o^2 \sin^2 \phi + n_e^2 \cos^2 \phi)^{1/2}} - n_o. \quad (13)$$

In these expressions  $\delta$  is the optical phase retardation given by the cell,  $\Delta n_{\text{eff}}$  is the effective birefringence,  $n_o$ ,  $n_e$  are the ordinary/extraordinary refractive indices and  $\phi$  is the angle between the director and the incident light. If  $\psi(x, y)$  is varying randomly, the average intensity  $I \equiv \langle I((x, y)) \rangle$  can be written as

$$I = \frac{1}{2} I_0 \sin^2 \left( \frac{\pi d \Delta n_{\text{eff}}}{\lambda} \right) \quad (14)$$

because  $\langle \sin 2\psi(x, y) \rangle = 1/2$  when averaged in two dimensions. Equation (14) does not, in general, give a dark field-free state (except when the  $d\Delta n_{\text{eff}}$  combination would make the cell approximate to a lambda plate), but yields a certain brightness. The point is, however, that the birefringence is not changed when the first electro-optic process is activated by applying an electric field, because an induced tilt still gives the same randomness to  $\psi(x, y)$  in equation (11) and is averaged out. Thus, any electro-optic modulation measured on a random sample stems from the field dependence of the effective birefringence  $\Delta n_{\text{eff}}(E)$ . In earlier work [37] we have also shown that for changes in this parameter, a field-induced tilt or apparent tilt, has only a very small effect.



Generally speaking, the two sine-squared factors in equation (11) are functions of the electric field, because  $\psi$  and  $\delta$  are field dependent. For a perfectly oriented  $C_a^*$  phase in the bookshelf geometry,  $\psi(x, y, E) = \psi(E)$ , whereas the retardation  $\delta$  is independent of the direction of the optic axis and therefore field independent. This is a case of our first, linear electro-optic effect, where the optic axis reorientation results in a modulation of the same frequency  $f$  as that of the applied field. The intensity signal here reflects the field and frequency dependence of  $\psi$ ,

$$I \sim \sin^2 2\psi(E, f). \quad (15)$$

The random sample represents the other extreme, where only the second factor comes into play,

$$I \sim \sin^2 \alpha \Delta n_{\text{eff}}(E, f) \quad (16)$$

expressing ( $\alpha$  being a constant factor) the field and frequency dependence of the effective birefringence. Applying an electric field of frequency  $f$ , the birefringence changes ( $\delta \Delta n \sim E^2$ ) result in light intensity modulation of frequency  $2f$ . Because this second electro-optic effect is quadratic, it could also have been detected in the presence of the first effect by using lock-in techniques.

The random  $C_a^*$  sample was obtained by rapid cooling from the isotropic phase without any rubbing or shearing involved. The electro-optic modulation by this sample is, as expected, much smaller than in the case of the homogeneously aligned  $C_a^*$ , but still easy to follow. Normalized to the same relative values as for the first electro-optic mode, the second mode is found to be much slower, with a cut-off frequency at about 1 kHz. This coincides with the dielectrically active relaxation frequency of the  $P_L$  process for the same material at the same temperature. Thus, from electro-optic measurements we have been able to relate both  $P_H$  and  $P_L$  to optically active processes with the same characteristic frequencies. In fact, if the  $P_L$  peak was connected with the molecular rotation around the short axis, an electro-optic effect would not be exhibited. Conversely, the electro-optic effect shows that this is a collective excitation. Our previous designation of this as collective helicoidal fluctuations is in good agreement with the fact that such fluctuations are coupled to weak changes in the effective value of  $\Delta n$ .

## 6. Conclusions

The dielectric spectrum of the antiferroelectric phase has its finger print in the appearance of two well separated absorption peaks  $P_L$  and  $P_H$ . The temperature dependence of  $\varepsilon$  and  $f_R$  of the  $P_L$  and  $P_H$  absorptions, their evolution with bias field, and electro-optic measurements give strong indications that these two processes cannot be attributed, as repeatedly stated in the literature

[7, 16, 23], to the molecular reorientation around the short axis and soft mode, respectively. Instead, however, we propose that the  $P_H$  process is connected to the collective reorientation of the molecules in two adjacent smectic layers in an *opposite* direction and the  $P_L$  process to the collective phase fluctuations (Goldstone mode) associated with the helicoidal superstructure. We would like to add that some authors [20] have observed a low frequency process which has been attributed to an anti-phase mode. This process shows a maximum in the dielectric strength at the  $C_\gamma^* - C_a^*$  phase transition.

If the antiferroelectric material has an overlying ferroelectric phase, the strong ferroelectric Goldstone mode from that phase will appear as an additional peak in at least one of the low-lying phases in a frequency range not far from  $f_L$ . A weaker ferroelectric Goldstone mode peak may also occur in the  $C_a^*$  phase due to the adjacent  $C_\gamma^*$  phase. In general, non-characteristic peaks may appear in adjacent phases due to the coexistence of phases across first order transitions. Several such peaks may appear in a phase like  $C_\gamma^*$  which is bounded by a first order transition on either side ( $C_a^* - C_\gamma^* - C^*$ ). In the narrow ferroelectric phase, the amount of information obtainable is limited, but two corresponding peaks appear. The low frequency peak can be identified with the expected Goldstone mode, whereas the high frequency mode can be observed to continue into the antiferroelectric high frequency mode at the onset of the  $C_\gamma^* - C_a^*$  transition and probably, like this latter process, is a kind of anti-phase mode in the azimuthal angle, and not a soft mode in the tilt angle.

## References

- [1] MEYER, R. B., LIEBERT, L., STRZELECKI, L., and KELLER, P., 1975, *J. Phys. (Paris) Lett.*, **36**, L-96.
- [2] CLARK, N. A., and LAGERWALL, S. T., 1980, *Appl. Phys. Lett.*, **36**, 899.
- [3] GAROFF, S., and MEYER, R. B., 1977, *Phys. Rev. Lett.*, **38**, 848.
- [4] CHANDANI, A. D. L., HAGIWARA, T., SUZUKI, Y., OUCHI, Y., TAKEZOE, H., and FUKUDA, A., 1988, *Jpn. J. appl. Phys.*, **27**, L729; TAKEZOE, N., LEE, J., OUCHI, Y., and FUKUDA, A., 1991, *Mol. Cryst. liq. Cryst.*, **202**, 85.
- [5] ZEKS, B., and CEPIC, M., 1993, *Liq. Cryst.*, **14**, 445; CEPIC, M., and ZEKS, B., 1996, *Ibid.*, **20**, 29.
- [6] We are using the notation  $C_a^*$  for the antiferroelectric phase, rather than  $C_A^*$ . There are two reasons for this. Firstly, capital letters are used in describing differences in smectic order, like smectic A, B, C ... Being a tilted smectic, the  $C_a^*$  has absolutely nothing to do with the orthogonal smectic  $A^*$  as the notation might suggest. Secondly, the property of being optically uniaxial does not relate the phase to smectic  $A^*$  any more than would be the case for a short pitch smectic  $C^*$  which is also uniaxial. The use of  $C_a^*$  is also in accordance with the lower case index letters used in  $C_\alpha^*$  and  $C_\gamma^*$ . Finally the index a in  $C_a^*$  should not be interpreted as an abbreviation for 'antiferroelectric' but for 'alternating tilt'

- or anti-tilt. In this way, the notation  $C_a$  for the non-chiral phase also makes sense, as  $C_a$  then represents a non-chiral tilted smectic with alternating tilt. This phase, of course has no antiferroelectric properties.
- [7] FUKUI, M., ORIHARA, H., SUZUKI, A., ISHIBASHI, Y., YAMADA, Y., YAMAMOTO, N., MORI, K., NAKAMURA, K., SUZUKI, Y., and KAWAMURA, I., 1990, *Jpn. J. appl. Phys.*, **29**, L329.
- [8] ROSARIO DE LA FUENTE, M., MERINO, S., GONZALEZ, Y., PEREZ JUBINDO, M. A., ROS, B., PUERTOLAS, J. A., CASTRO, M., 1995, *Adv. Mater.*, **7**, 564.
- [9] TAKEZOE, H., LEE, J., OUCHI, Y., and FUKUDA, A., 1991, *Mol. Cryst. liq. Cryst.*, **85**,
- [10] OSTROVSKI, B. I., RABINOVICH, A. Z., SONIN, A. S., STRUKOV, B. A., and TARASKIN, S. A., 1978, *Ferroelectrics*, **20**, 189.
- [11] HOFFMANN, J., KUCZYNSKI, W., and MALECKI, J., 1978, *Mol. Cryst. liq. Cryst.*, **44**, 287.
- [12] GLOGAROVA, M., FOUSEK, J., LEJCEK, L., and PAVE, J., 1984, *Ferroelectrics*, **58**, 161.
- [13] FILIPIC, C., CARLSSON, T., LEVSTIK, A., ZEKS, B., BLINC, R., GOUDA, F., LAGERWALL, S. T., and SKARP, K., 1988, *Phys. Rev. A*, **38**, 5833.
- [14] BIRDAR, A. M., WROBEL, S., and HAASE, W., 1989, *Phys. Rev. A*, **39**, 2693.
- [15] KREMER, F., SCHÖNFELD, A., HOFMAN, A., ZENTEL, R., and POTHS, H., 1992, *Polym. Adv. Techn.*, **3**, 249.
- [16] HIRAOKA, K., TAGUCHI, A., OUCHI, Y., TAKEZOE, H., and FUKUDA, A., 1990, *Jpn. J. appl. Phys.*, **29**, L103.
- [17] ISOZAKI, T., SUZUKI, Y., KAWAMURA, I., MORI, K., YAMADA, N., ORIHARA, H., and ISHIBASHI, Y., 1991, *Jpn. J. appl. Phys.*, **30**, L1573.
- [18] OKABE, N., SUZUKI, Y., KAWAMURA, I., ISOZAKI, T., TAKEZOE, H., and FUKUDA, A., 1992, *Jpn. J. appl. Phys.*, **31**, L793.
- [19] GLOGAROVA, M., SVERENYAK, H., NGUYEN, H. T., and DESTRADE, C., 1993, *Ferroelectrics*, **147**, 43.
- [20] GISSE, P., PAVEL, J., NGUYEN, H. T., LORMAN, V. L., 1993, *Ferroelectrics*, **147**, 27.
- [21] CEPIC, M., HEPPKE, G., HOLLIDT, J.-M., LÖTZSCH, D., ZEKS, B., 1993, *Ferroelectrics*, **147**, 159.
- [22] SARALA, S., ROY, A., MADHUSUDANA, N. V., NGUYEN, H. T., DESTRADE, C., and CLUZEAU, P., 1995, *Mol. Cryst. liq. Cryst.*, **261**, 1
- [23] MORITAKE, H., UCHIYAMA, Y., MYOJIN, K., OZAKI, M., and YOSHINO, K., 1993, *Ferroelectrics*, **147**, 53.
- [24] HIRAOKA, K., TAKEZOE, H., and FUKUDA, A., 1993, *Ferroelectrics*, **147**, 13.
- [25] HILLER, S., PIKIN, S. A., HASSE, W., GOODBY, J. W., and NISHIYAMA, I., 1994, *Jpn. J. appl. Phys.*, **33**, L1170.
- [26] BUIVYDAS, M., GOUDA, F., LAGERWALL, S. T., and STEBLER, B., 1995, *Liq. Cryst.*, **18**, 879.
- [27] HILLER, S., PIKIN, S. A., HASSE, W., GOODBY, J. W., and NISHIYAMA, I., 1994, *Jpn. J. appl. Phys.*, **33**, L1096.
- [28] PANARIN, Y. P., XU, H., MACLUGHADHA, S. T., VIJ, J. K., SEED, A. J., HIRD, M., and GOODBY, J. W., 1995, *J. Phys. condens. Matter*, **7**, L351.
- [29] BÖMELBURG, J., HEPPKE, G., KOMITOV, L., LAGERWALL, S. T., and STEBLER, B., 1996, *Ferroelectrics*, **178**, 267.
- [30] GOUDA, F., DAHLGREN, A., LAGERWALL, S. T., STEBLER, B., BÖMELBURG, J., and HEPPKE, G., 1996, *Ferroelectrics*, **178**, 187.
- [31] GESTBLOM, B., and NORELAND, E., 1977, *J. chem. Phys.*, **81**, 782.
- [32] KRESSE, H., 1983, *Advances in Liquid Crystals*, **6**, 109.
- [33] PFEIFFER, M., SOTO, G., WROBEL, S., and HASSE, W., 1991, *Ferroelectrics*, **121**, 55.
- [34] HIRAOKA, K., CHANDANI, A. D. L., GORECKA, E., OUCHI, Y., TAKEZOE, H., and FUKUDA, A., 1990, *Jpn. J. appl. Phys.*, **29**, L1473.
- [35] JONES, J. C., and RAYNES, E. P., 1992, *Liq. Cryst.*, **11**, 199.
- [36] GOUDA, F., LAGERWALL, S. T., SKARP, K., STEBLER, B., KREMER, F., and VALLERIEU, S. U., 1994, *Liq. Cryst.*, **17**, 367.
- [37] BUIVYDAS, M., GOUDA, F., LAGERWALL, S. T., MATUSZCZYK, M., and STEBLER, B., 1995, *Ferroelectrics*, **166**, 195.